Cardiovasc Intervent Radiol (2023) 46:240–248
https://doi.org/10.1007/s00270-022-03353-2

CLINICAL INVESTIGATION STROKE/NEUROINTERVENTIONS

Low Wall Shear Stress and High Intra-aneurysmal Pressure are Associated with Ruptured Status of Vertebral Artery Dissecting Aneurysms

Heng Wei[1] · Kun Yao[2] · Qi Tian[1] · Shoumeng Han[1] · Wenhong Gao[2] · Wenrui Han[1] · Sheng Liu[1] · Guijun Wang[1] · Qianxue Chen[1] · Mingchang Li[1]

Received: 18 April 2022 / Accepted: 26 December 2022 / Published online: 18 January 2023

Abstract

Purpose The morphological and hemodynamic features of patients with vertebral artery dissecting aneurysms (VADAs) are yet unknown. This study sought to elucidate morphological and hemodynamic features of patients with ruptured and unruptured VADAs based on computed flow simulation.

Methods Fifty-two patients (31 unruptured and 21 ruptured VADAs) were admitted to two hospitals between March 2016 and October 2021. All VADAs were located in the intradural segment, and their clinical, morphological, and hemodynamic parameters were retrospectively analyzed. The hemodynamic parameters were determined through computational fluid dynamics simulations. Univariate statistical and multivariable logistic regression analyses were employed to select significantly different parameters and identify key factors. Receiver operating characteristic (ROC) analysis was used to assess the discrimination for each key factor.

Results Four hemodynamic parameters were observed to significantly differ between ruptured and unruptured VADAs, including wall shear stress (WSS), low shear area, intra-aneurysmal pressure (IAP), and relative residence time. However, no significant differences were observed in morphological parameters between ruptured and unruptured VADAs. Multivariable logistic regression analysis revealed that low WSS and high IAP were significantly observed in the ruptured VADAs and demonstrated adequate discrimination.

Conclusions This research indicates significant hemodynamic differences, but no morphological differences were observed between ruptured and unruptured VADAs. The ruptured group had significantly lower WSS and higher IAP than the unruptured group. To further confirm the roles of low WSS and high IAP in the rupture of VADAs, large prospective studies and long-term follow-up of unruptured VADAs are required.

Keywords Computational fluid dynamic · Morphological · Hemodynamic · Vertebral artery dissecting aneurysms

Introduction

Vertebral artery dissecting aneurysms (VADAs) refer to a tear in the vertebral artery that results in an intramural hematoma and/or an aneurysmal dilatation, accounting for an average annual incidence rate of approximately 0.97–1.5 cases per 100 people [1]. Currently, the etiology of VADAs remains unclear, and most literature believes that they occur spontaneously, while other reports speculate that a potentially fatal arterial injury causes them during sports [2, 3]. VADAs present with symptoms of posterior circulation ischemia due to vertebrobasilar artery

Heng Wei and Kun Yao have contributed equally to this study.

✉ Mingchang Li
mingcli@whu.edu.cn

[1] Department of Neurosurgery, Renmin Hospital of Wuhan University, 99 Ziyang Road, Wuhan 430060, Hubei Province, China

[2] Department of Neurosurgery, Jingzhou Central Hospital, Jingzhou 434020, China

ischemia and brain stem compression or with subarachnoid hemorrhage, resulting in high morbidity and mortality [4]. Due to the risks associated with surgical treatment of unruptured VADAs and the high mortality associated with ruptured VADAs, deciding which aneurysms require preventive treatment can be a dilemma. Therefore, it is critical to accurately predict rupture risk in VADAs.

Numerous researches have been conducted on the rupture risk of intracranial aneurysms, but prediction accuracy remains far from ideal [5]. Many studies existed on the relationship between morphological and hemodynamic parameters with the rupture risk of saccular aneurysms [6, 7], but they have not been reported on VADAs. Hemodynamics have been demonstrated to be crucial for forming, growing, and rupturing saccular intracranial aneurysms [8]. This study aimed to identify morphological and hemodynamic differences between ruptured and unruptured intradural VADAs based on computed flow simulation to guide the treatment strategy of unruptured VADAs.

Material and Methods

Patient Selection

All patient's data were retrospectively reviewed, including imaging data and medical records from the electronic medical record system in two medical research centers. The data were collected from 52 consecutive patients diagnosed with intradural segment VADAs from March 2016 to October 2021. The intradural segment refers to the vertebral artery from the foramen magnum to the origin of basilar artery [9]. Cerebral digital subtraction angiography (DSA) was performed on all VADAs and combined with computed tomography angiography and high-resolution magnetic resonance imaging for accurate diagnosis and preoperative evaluation. Two neurosurgeons with over 10-year experience in interpreting cerebral angiograms and the endovascular treatment of intracranial aneurysms confirmed the findings. This study was approved by the Clinical Research Ethics Committee of the two Hospitals.

Inclusion criteria included (1) aneurysm located in the intradural segment of the vertebral artery and (2) dissecting aneurysm. Exclusion criteria were as follows: (1) saccular aneurysms; (2) aneurysm located in the extracranial segment of the vertebral artery; (3) combined with moyamoya disease, vascular malformations, or traumatic aneurysms; (4) multiple aneurysms; and (5) images with poor quality for morphology measurement or computational fluid dynamics.

Patient Groups

Patients were divided into rupture and non-rupture groups based on the presence of subarachnoid hemorrhage. Subarachnoid hemorrhage was confirmed by brain computed tomography and clinical condition. Lumbar puncture was considered mandatory to confirm the diagnosis in cases where subarachnoid hemorrhage was suspected clinically, but brain computed tomography was negative. The results were confirmed by two neurosurgeons with over 10-year experience in aneurysm diagnosis and treatment.

Aneurysm Modeling

Transfemoral artery catheterization was used for all catheter angiographies. All three-dimensional (3D) images were obtained through DSA using a Siemens angiographic system (Siemens Healthineers, Forchheim, Germany). Rotational angiograms were performed 2 s after 5-s contrast injection, with 18 ml of contrast agent at a rate of 3 ml/s and a 200° rotation. 3D-DSA data were imported into Mimics medical 21.0 (Materialise, Belgium) to perform segmentation and obtain the preliminary 3D models and then imported into 3-matic medical 13.0 (Materialise, Belgium) for model repair and smoothing. The software ANSYS Fluent 2021 R2 and CFD-post 2021 R2 (ANSYS Inc., USA) were used to simulate hemodynamics and calculate the value of each hemodynamic parameter. Software settings are available in the online supplement. Finally, the calculation time was set to last for three cardiac cycles, with the result of the third cycle reaching a stable state after 200-time steps. The blood vessel was modeled as a rigid wall, and the blood flow was modeled as an incompressible Newtonian fluid with constant temperature and laminar flow, resulting in Navier–Stokes equation approximate blood flow.

Morphology Analysis

The 3D model of VADAs and parent artery could be freely rotated and measured in our workplace system, as the observers found the best view angle to measure morphological variables. The multiple morphological parameters used in this study included maximum length of the aneurysm (Lmax), maximum diameter of the aneurysm (Wmax), the average value of parent artery diameter at the proximal part of the aneurysm (Dp1), and the average value of parent artery diameter at the distal part of the aneurysm (Dp2), and the average value of parent artery diameter (Dp = (Dp1 + Dp2)/2). Besides, we analyzed the following ratios related to aneurysm shape, including Lmax/Wmax, Lmax/Dp, and Wmax/Dp. The morphological parameters used in this study are described briefly in

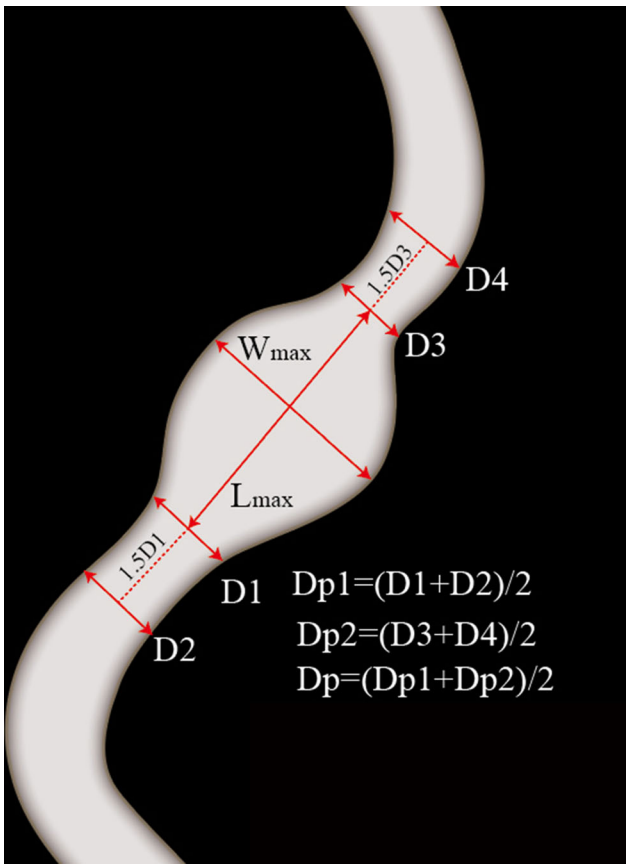

Fig. 1 Schematic diagram for the measurement of vertebral artery dissecting aneurysms and illustration of morphological parameters

Fig. 1. The parameters were determined by two independent observers blinded to information pertaining to subarachnoid hemorrhage under the supervision of an experienced neurosurgeon.

Hemodynamic Analysis

Nine hemodynamic parameters were defined based on aneurysm surface and volume: wall shear stress (WSS), intra-aneurysmal pressure (IAP), normalized WSS, WSS gradient, low shear area, oscillatory shear index, relative residence time, normalized pressure, and combined hemodynamic parameters. WSS refers to the tangential, frictional stress caused by the action of blood flow on the vessel wall. IAP is the force energy with which blood hits the inner wall of the aneurysm sac. Normalized WSS represents the ratio of the aneurysm wall shear force to the mean value of the parent artery wall shear force. WSS gradient indicates the amplitude of variation along the wall shear force direction. The low shear area was described by the area of aneurysm wall exposed to WSS below 10% of the mean WSS of the parent artery. Oscillatory shear index indicates WSS magnitude fluctuations and describes the tangential force oscillation as a function of the cardiac cycle. Relative residence time characterizes the stagnation time of blood flow around the vascular wall. Normalized pressure represented the ratio of the pressure in the aneurysm sac to the pressure in the parent artery and was used to compare IAP of different aneurysms. Combined hemodynamic parameters were the weighted average value of normalized WSS and normalized oscillatory shear index. All hemodynamic parameters were defined and calculated according to previous studies [10–14].

Statistical Analysis

All data were analyzed using IBM SPSS Statistics version 25.0 (SPSS, Inc., Chicago, Illinois, US). Continuous variables were analyzed using independent t test or Mann–Whitney U test and presented as mean ± standard deviation or median with interquartile range, respectively. Categorical variables were expressed as numbers and were analyzed using χ^2 tests. Differences were considered statistically significant if the two-tailed P values were < 0.05. Statistically significant variables in univariate analysis were further evaluated using binary logistic regression analysis to identify independent risk factors. Receiver operating characteristic (ROC) curve and area under curve (AUC) were performed to assess discriminatory capabilities.

Results

Patient's Clinical Characteristics

Of 52 VADAs, 21 were ruptured, and 31 were unruptured. The average age of ruptured group was 55.10 ± 9.24 years, including 12 males and 9 females, while that of unruptured group was 53.74 ± 12.68 years, including 16 males and 15 females. The onset symptoms of patients in the unruptured group were ipsilateral neck pain in 12 patients, headache in 9 patients, and vertigo in 6 patients. There were no significant differences in age, gender, smoking, drinking, hypertension, diabetes, coronary heart disease, or hyperlipidemia between the two groups (Table 1).

Univariate Statistical Analysis of Morphologic Factors Between Ruptured and Unruptured VADAs

By comparing morphological parameters between ruptured and unruptured VADAs, we found that Wmax, Lmax, Dp1, Dp, Lmax/Dp, and Wmax/Dp in the ruptured group were lower than in the unruptured group, while Dp2 and Lmax/Wmax were higher in the ruptured group. However, all

Table 1 Clinical characteristics between ruptured and unruptured VADAs

Variable	Ruptured	Unruptured	*P* value
Age (year)	55.10 ± 9.24	53.74 ± 12.68	0.677
Gender			
Male	12	16	0.781
Female	9	15	
Hypertension			
Yes	14	19	0.774
No	7	12	
Diabetes			
Yes	3	2	0.383
No	18	29	
Coronary heart disease			
Yes	2	1	0.558
No	19	30	
Hyperlipidemia			
Yes	2	5	0.687
No	19	26	
Drinking			
Yes	3	2	0.383
No	18	29	
Smoking			
Yes	5	6	0.739
No	16	25	

VADAs vertebral artery dissecting aneurysms

$P < 0.05$ was considered significant

Table 2 Results of univariate statistical analysis for morphological characteristics between ruptured and unruptured VADAs

Variable	Ruptured	Unruptured	*P* value
Wmax (mm)	6.80 (4.99, 8.22)	7.38 (6.32, 8.86)	0.154
Lmax (mm)	9.48 (7.97, 11.24)	10.12 (8.29, 12.37)	0.467
Dp1 (mm)	3.19 (2.83, 3.28)	3.12 (2.98, 3.35)	0.589
Dp2 (mm)	3.34 ± 0.49	3.32 ± 0.47	0.906
Dp (mm)	3.17 ± 0.52	3.24 ± 0.33	0.589
Lmax/Wmax	1.38 (1.23, 1.62)	1.32 (1.22, 1.50)	0.275
Lmax/Dp	3.15 ± 0.78	3.17 ± 0.82	0.952
Wmax/Dp	2.21 (1.62, 2.58)	2.34 (2.02, 2.58)	0.478

VADAs vertebral artery dissecting aneurysms, *Wmax* maximum diameter of the aneurysm, *Lmax* maximum length of the aneurysm, *Dp1* the average value of parent artery diameter at the proximal part of the aneurysm, *Dp2* the average value of parent artery diameter at the distal part of the aneurysm, $\underline{Dp}$ the average value of parent artery diameter

$P < 0.05$ was considered significant

morphological parameters presented no significant statistical differences between the two groups (Table 2).

Univariate Statistical Analysis of Hemodynamic Factors Between Ruptured and Unruptured Vadas

Nine hemodynamic parameters of VADAs were analyzed (Figs. 2, 3). Low shear area ($P = 0.002$), IAP ($P < 0.001$), and relative residence time ($P = 0.028$) in the ruptured group were significantly higher than those in the unruptured group. WSS ($P < 0.001$) in the ruptured group was significantly lower than that in the unruptured group, while the other five hemodynamic parameters were not significantly different between the two groups (Table 3).

Multivariable Logistic Regression Analysis and ROC Analysis

We performed binary logistic regression analysis on the four significant hemodynamic parameters and found that IAP (OR = 1.019, 95% CI 1.006–1.034, $P = 0.006$) and WSS (OR = 0.085, 95% CI 0.018–0.394, $P = 0.002$) were independent risk factors for VADA rupturing. The result indicated that ruptured VADAs had lower WSS and higher IAP than unruptured VADAs (Table 4).

ROC curve analysis revealed that WSS (AUC = 0.802, 95% CI 0.682–0.922) and IAP (AUC = 0.782, 95% CI 0.652–0.912) provided adequate discrimination between ruptured and unruptured VADAs.

Discussion

In this study, by comparing eight morphological and nine hemodynamic parameters of intradural VADAs, no differences in morphological parameters were found between ruptured and unruptured VADAs, but ruptured VADAs had significantly lower WSS and higher IAP. This difference in hemodynamics may be critical to understanding the mechanism of VADA rupture and formulating treatment strategies for unruptured VADAs.

Clinical presentations of VADAs can be categorized into three groups: posterior circulation ischemia or infarction, acute subarachnoid hemorrhage, and posterior fossa mass effect on the brain stem or cranial nerve [15]. Although long-term follow-up of patients with unruptured VADAs has revealed that prognosis is good regardless of conservative treatment or endovascular treatment, patients with ruptured VADAs have poor prognosis without surgery or endovascular intervention [16]. In the bleeding VADAs group, the mortality rate was 50% in the untreated group [17]. Patients have high mortality and morbidity even with surgical or endovascular treatment in the case of

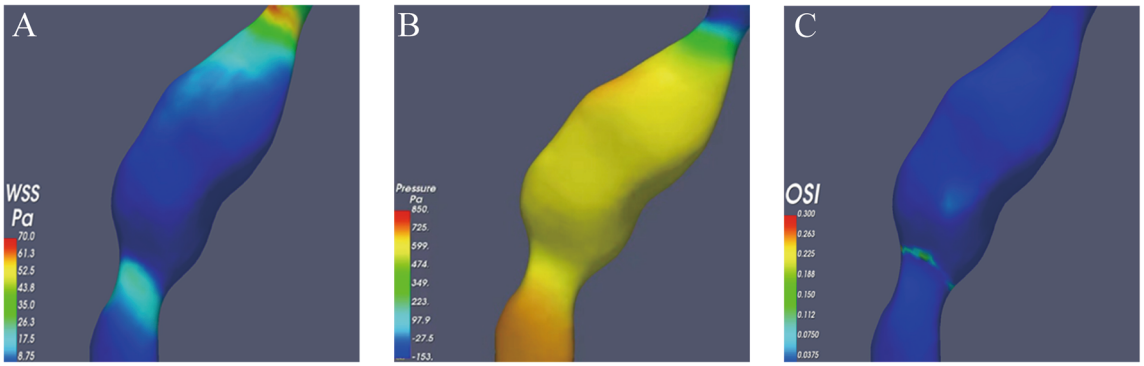

Fig. 2 Hemodynamic analysis of ruptured vertebral artery dissecting aneurysms. **A** Wall shear stress. **B** Intra-aneurysmal pressure. **C** Oscillatory shear index. Different colors indicate different levels of hemodynamic parameters; red corresponds to high value of parameter and blue corresponds to low value of parameter

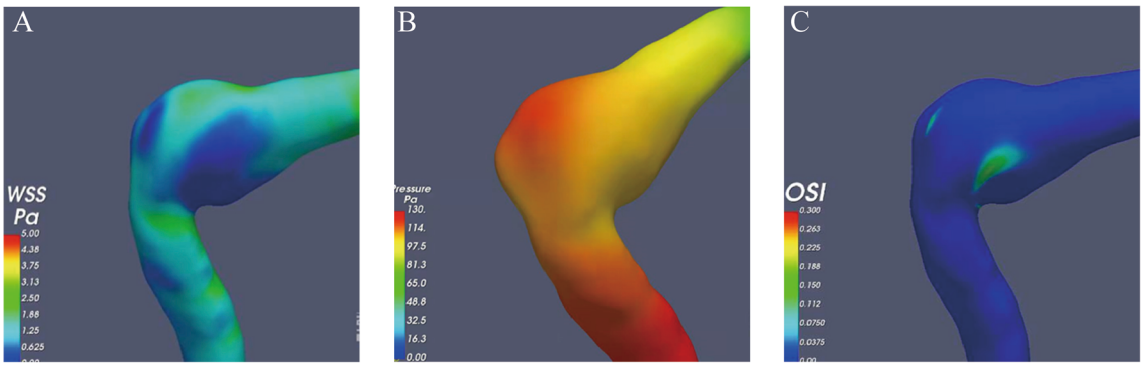

Fig. 3 Hemodynamic analysis of unruptured vertebral artery dissecting aneurysms. **A** Wall shear stress. **B** Intra-aneurysmal pressure. **C** Oscillatory shear index. Different colors indicate different levels of hemodynamic parameters; red corresponds to high value of parameter, and blue corresponds to low value of parameter

Table 3 Results of univariate statistical analysis for hemodynamic characteristics between ruptured and unruptured VADAs

Variable	Ruptured	Unruptured	*P* value
WSS (Pa)	1.70 ± 0.67	2.59 ± 0.81	< 0.001
Normalized WSS	0.49 ± 0.16	0.57 ± 0.15	0.055
WSS gradient	118.89 (102.84, 139.93)	104.34 (89.47, 126.33)	0.085
Normalized pressure	1.29 (1.24, 1.36)	1.25 (1.17, 1.35)	0.168
Oscillatory shear index	0.018 ± 0.007	0.020 ± 0.008	0.400
Combined hemodynamic parameters	0.16 ± 0.04	0.16 ± 0.05	0.952
Relative residence time (s)	0.90 ± 0.21	0.76 ± 0.22	0.028
Low shear area	0.24 (0.19, 0.38)	0.15 (0.11, 0.22)	0.002
IAP (Pa)	369.20 ± 83.93	287.69 ± 66.47	< 0.001

VADAs vertebral artery dissecting aneurysms, *WSS* wall shear stress, *IAP* intra-aneurysmal pressure

$P < 0.05$ was considered significant

hemorrhagic rupture due to the specific anatomical relationship between the aneurysm and the brain stem [18]. The risk of postoperative cerebral infarction or rebleeding remains higher than for saccular aneurysms [19]. Meanwhile, VADAs not prone to rupture are sometimes surgically manipulated, with a risk of complication. Therefore, active surgical or endovascular treatment of unruptured aneurysms with high rupture risk and dynamic follow-up of aneurysms with low rupture risk may be a better choice. Accordingly, accurately assessing the rupture risk of VADAs and formulating reasonable treatment strategies are considered to be the keys to managing unruptured VADAs.

Table 4 The results of multivariable logistic regression analysis for significant variables

Variable	OR (95% CI)	*P* value
WSS	0.085 (0.018, 0.394)	0.002
Low shear area (× 10)	2.457 (0.975, 6.189)	0.057
Relative residence time (× 10)	1.437 (0.892, 2.313)	0.136
IAP	1.019 (1.006, 1.034)	0.006

OR odds ratio, *CI* confidence interval, *WSS* wall shear stress, *IAP* intra-aneurysmal pressure

$P < 0.05$ was considered significant

Previous studies have confirmed that clinical characteristics are closely linked to the rupture risk of intracranial aneurysms. Our study demonstrated that clinical characteristics of age, sex, smoking, drinking, diabetes, hyperlipidemia, coronary heart disease, and hypertension exhibited no significant difference between the two groups, suggesting comparable morphological and hemodynamic results. Due to more complicated and tedious collection and calculation of hemodynamic parameters, the role of morphological parameters is important in predicting the rupture risk of aneurysm. Prior studies in intracranial aneurysm literature have found that size, aspect ratio, and size ratio are associated with intracranial aneurysm rupture [20, 21]. However, these results were all based on saccular aneurysms. In this study, eight morphological parameters that may be applicable to VADAs were used for statistical analysis between ruptured and unruptured VADAs, and the result revealed that none of morphological parameters correlated with rupture status. These findings imply that it may be inappropriate to classify the rupture risk of VADAs using morphological parameters previously utilized for saccular intracranial aneurysms. VADAs often involve the whole circumference of vertebral artery and lack a defined neck. The dilation of dissecting aneurysm is not only perpendicular to the parent artery but also along the parallel direction of the parent artery, showing a variety of shapes such as a string and pearl pattern, fusiform pattern or double lumen signs on imaging [22, 23]. The growth direction of saccular aneurysms is mainly perpendicular to the parent artery. This morphological difference may be one of the reasons for the inconsistency in the rupture risk associated with morphological parameters between dissecting and saccular aneurysms. In future, we must find personalized morphological parameters suitable for VADA rupture risk studies. Previous studies have reported that steep vertebral artery of the dissecting side, basilar artery bending < 3 mm, and pearl-and-string sign may be associated with ruptured risk of intradural VADAs [24]. However, these results still need to be confirmed by further research.

Hemodynamics are important in the pathogenesis, progression, and rupture of cerebral aneurysms. WSS was a hemodynamic parameter widely studied in saccular intracranial aneurysms and proposed as an important hemodynamic parameter of computational fluid dynamics-based studies. Although a few researchers have suggested that saccular aneurysms with high WSS were more likely to rupture, more studies support lower WSS as a risk factor for saccular aneurysm rupture. Xiang et al. compared the hemodynamics of ruptured and unruptured aneurysms and found that lower WSS was associated with rupture status of intracranial aneurysms [10]. Miura et al. compared morphological and hemodynamic characteristics of 106 middle cerebral artery aneurysms and found that only lower WSS was significantly associated with rupture status of aneurysms [25]. In this study, we identically found significantly lower WSS associated with the rupture status of VADAs. Our results suggest that the mechanism by which WSS acts on saccular aneurysms and causes their rupture may also apply to intradural VADAs. The mechanism of aneurysm rupture caused by low WSS may be correlated with activating inflammatory cell-mediated destructive remodeling of the vessel wall [26, 27]. Low WSS promotes endothelial cell disorders and changes endothelial cell secretion patterns, leading to increased vasoconstriction and production of inflammatory substances, as well as decreased vasodilators and antioxidants [8]. Low WSS also upregulates endothelial surface adhesion molecules, causing blood flow-induced nitrous oxide dysfunction, and increased endothelial permeability, thereby promoting atherosclerosis and inflammatory cell infiltration. These inflammatory infiltrates produce large amounts of matrix metalloproteinases to degrade the extracellular matrix, disrupting vascular integrity and promoting aneurysm growth and rupture [28, 29].

The impact of blood flow on the vessel wall will form three different directions of physiological pressure. The first is WSS, the second is the transmural pressure (the pressure of intravascular blood acting perpendicularly to the vascular wall), and the third is the mechanical stretch [30]. IAP is an inertial force acting perpendicularly to the aneurysm wall, which is converted from the kinetic energy of blood. Local blood flow converts fluid kinetic energy into transmural pressure perpendicular to the vessel wall at the area of flow impingement [31]. In previous research, IAP was measured by inserting an arterial pressure transducer into the local area of the aneurysm and always in the dome [32]. However, aneurysm rupture is not always at the aneurysm dome, and this operation itself may have bias, such as the definition of aneurysm dome. Aneurysm rupture results from multifactorial influence on the overall

progression of the aneurysm, and during the process of growth and rupture, not only the dome of aneurysm wall degenerates. Previous studies have also found that local aneurysm pressure elevation is not a key factor in aneurysm rupture [33]. Therefore, measuring local area IAP with a pressure transducer may cause a deviation in the results. Computational fluid dynamics method can simulate the hemodynamics of whole aneurysms and parent arteries throughout the cardiac cycle by setting appropriate boundary conditions, which could more accurately reflect the transmural pressure of blood flow on the arterial wall. Hassan et al. have found that high IAP may induce enlargement of vertebrobasilar saccular aneurysms since high IAP may be linked to the risk of saccular aneurysm rupture [34]. Cebral et al. analyzed the hemodynamics of ruptured and unruptured aneurysms after being treated with flow-diverting stents and found that IAP increased significantly in the rupture group [35]. Suzuki et al. also found that the maximum pressure areas corresponded with the thin-walled regions of cerebral aneurysms [36]. Previous research reported that high IAP could also lead to rupture of aortic dissecting aneurysms [37]. Our findings indicate a statistically significant difference in IAP between ruptured and unruptured VADAs, and ROC curve analysis shows that AUC = 0.782 (P = 0.006). The results suggest that high IAP is related to VADA rupture and may be a potential parameter for predicting VADA rupture risk. At present, the mechanism of VADA rupture remains unclear. Previous studies have revealed that the rupture of VADAs is associated with high IAP induced by intramural hematoma, as the mechanical energy of high IAP leads to the tear of vertebral artery adventitia. Blood flows into the ruptured internal elastic lamina to form a hematoma, and the growing hematoma itself can alter the hemodynamics of aneurysm and the parent artery. The persistently enlarged false lumen narrows the true lumen of the parent artery, increasing resistance to blood flow through the true lumen. Simultaneously, once the adventitia is dilated, blood is more inclined to enter the dilated false lumen. These series of changes intensify blood flow into the false lumen. With the continuous increasing blood flow into the false lumen, the hematoma causes the adventitia to dilate distally. Finally, the adventitia cannot withstand the increased IAP, causing VADA to rupture at the most distended area [38–40]. Previous studies have shown that the flow-diverting stents and stent-assisted coiling embolization, which reduce the blood flow into the sac of aneurysms, are effective treatment for VADAs [41].

Some potential limitations existed in our study. First, although we selected patients from two centers, the number of cases remains small due to the low incidence of VADAs, which may have a deviation from the trial's results. Additional multi-center studies with larger samples are required to corroborate our results. Second, while several studies exist on morphological parameters in saccular aneurysms but few on dissecting aneurysms, the selected morphological parameters may be incomprehensive or imprecise. Third, this study was a retrospective analysis using a patient-specific model in computational fluid dynamics simulation, but the boundary conditions were not patient-specific, and the hemodynamic simulation employed assumptions of laminar flow, Newtonian blood, and rigid wall; this may lead to inaccurate trial results. Fourth, some studies demonstrated that the morphology of ruptured aneurysms may change [42]. This may possibly have occurred in hemodynamics before and after aneurysm rupture [43]. However, it is difficult to conduct a prospective study on the rupture risk of aneurysms in patients.

Conclusions

We compared eight morphological and nine hemodynamic parameters between ruptured and unruptured intradural VADAs. We found no significant morphological parameter differences, but the ruptured group had significantly lower WSS and higher IAP. The result suggests that low WSS and high IAP are related to the rupture status of VADAs. The role of low WSS and high IAP in the rupture of VADAs must be further assessed in large prospective studies and long-term follow-up of unruptured VADAs.

Author Contributions HW, KY, WG, QC and ML contributed to the conception, design and drafted the manuscript. HW, QT, SH, WH, SL, GW contributed to data acquisition and data analysis, HW, KY, QC and ML made the article preparation, editing and review. All authors contributed to the article and approved the submitted version.

Funding This study was funded by National Natural Science Foundation of China (Grant Nos: 81971870 and 82172173).

Declarations

Conflict of interest The authors declare that they have no competing interests.

Ethical Approval All procedures performed in studies involving human participants were in accordance with the ethical standards of the institutional and/or national research committee and with the 1964 Helsinki declaration and its later amendments or comparable ethical standards. The retrospective study was approved by the Clinical Research Ethics Committee of Renmin Hospital of Wuhan University and Jingzhou Central Hospital.

Informed Consent Informed consent was obtained from all individual participants included in the study.

Consent for Publication Consent for publication was obtained for every individual person's data included in the study.

References

1. Pomeraniec IJ, Mastorakos P, Raper D, et al. Rerupture following flow diversion of a dissecting aneurysm of the vertebral artery: case report and review of the literature. World Neurosurg. 2020;143:171–9.
2. Choi MH, Hong JM, Lee JS, et al. Preferential location for arterial dissection presenting as golf-related stroke. AJNR Am J Neuroradiol. 2014;35(2):323–6.
3. Suzuki S, Tsuchimochi R, Abe G, et al. Traumatic vertebral artery dissection in high school rugby players: a report of two cases. J Clin Neurosci. 2018;47:137–9.
4. Guan J, Li G, Kong X, et al. Endovascular treatment for ruptured and unruptured vertebral artery dissecting aneurysms: a meta-analysis. J Neurointerv Surg. 2017;9(6):558–63.
5. Mangrum WI, Huston J 3rd, Link MJ, et al. Enlarging vertebrobasilar nonsaccular intracranial aneurysms: frequency, predictors, and clinical outcome of growth. J Neurosurg. 2005;102(1):72–9.
6. Xu L, Wang H, Chen Y, et al. Morphological and hemodynamic factors associated with ruptured middle cerebral artery mirror aneurysms: a retrospective study. World Neurosurg. 2020;137:e138–43.
7. Can A, Du R. Association of hemodynamic factors with intracranial aneurysm formation and rupture: systematic review and meta-analysis. Neurosurgery. 2016;78(4):510–20.
8. Meng H, Tutino VM, Xiang J, et al. HighWSS or LowWSS? Complex interactions of hemodynamics with intracranial aneurysm initiation, growth, and rupture: toward a unifying hypothesis. AJNR Am J Neuroradiol. 2014;35(7):1254–62.
9. Tay KY, U-King-Im JM, Trivedi RA, et al. Imaging the vertebral artery. Eur Radiol. 2005;15(7):1329–43.
10. Xiang J, Natarajan SK, Tremmel M, et al. Hemodynamic-morphologic discriminants for intracranial aneurysm rupture. Stroke. 2011;42(1):144–52.
11. Yuan J, Li Z, Jiang X, et al. Hemodynamic and morphological differences between unruptured carotid-posterior communicating artery bifurcation aneurysms and infundibular dilations of the posterior communicating artery. Front Neurol. 2020;11:741.
12. Cho KC, Choi JH, Oh JH, et al. Prediction of thin-walled areas of unruptured cerebral aneurysms through comparison of normalized hemodynamic parameters and intraoperative images. Biomed Res Int. 2018;2018:3047181.
13. Kursun B, Ugur L, Keskin G. Hemodynamic effect of bypass geometry on intracranial aneurysm: a numerical investigation. Comput Methods Progr Biomed. 2018;158:31–40.
14. Zhai X, Geng J, Zhu C, et al. Risk factors for pericallosal artery aneurysm rupture based on morphological computer-assisted semiautomated measurement and hemodynamic analysis. Front Neurosci. 2012;15:759806.
15. Yoon W, Seo JJ, Kim TS, et al. Dissection of the V4 segment of the vertebral artery: clinicoradiologic manifestations and endovascular treatment. Eur Radiol. 2007;17(4):983–93.
16. Yamada M, Kitahara T, Kurata A, et al. Intracranial vertebral artery dissection with subarachnoid hemorrhage: clinical characteristics and outcomes in conservatively treated patients. J Neurosurgery. 2004;101(1):25–30.
17. Rabinov JD, Hellinger FR, Morris PP, et al. Endovascular management of vertebrobasilar dissecting aneurysms. AJNR Am J Neuroradiol. 2003;24(7):1421–8.
18. Wang J, Sun Z, Bao J, Li Z, Bai D, Cao S. Endovascular management of vertebrobasilar artery dissecting aneurysms. Turk Neurosurg. 2013;23(3):323–8.
19. Takagi T, Takayasu M, Suzuki Y, et al. Prediction of rebleeding from angiographic features in vertebral artery dissecting aneurysms. Neurosurg Rev. 2007;30(1):32–9.
20. Xu WD, Wang H, Wu Q, et al. Morphology parameters for rupture in middle cerebral artery mirror aneurysms. J Neurointerv Surg. 2020;12(9):858–61.
21. Cui Y, Xing H, Zhou J, et al. Aneurysm morphological prediction of intracranial aneurysm rupture in elderly patients using four-dimensional CT angiography. Clin Neurol Neurosurg. 2021;208:106877.
22. Yamaura A, Ono J, Hirai S. Clinical picture of intracranial non-traumatic dissecting aneurysm. Neuropathol: Off J Jpn Soc Neuropathol. 2020;20(1):85–90.
23. Zenteno MA, Santos-Franco JA, Freitas-Modenesi JM, et al. Use of the sole stenting technique for the management of aneurysms in the posterior circulation in a prospective series of 20 patients. J Neurosurg. 2008;108(6):1104–18.
24. Matsukawa H, Shinoda M, Fujii M, et al. Differences in vertebrobasilar artery morphology between spontaneous intradural vertebral artery dissections with and without subarachnoid hemorrhage. Cerebrovasc Dis (Basel, Switz). 2012;34(5–6):393–9.
25. Miura Y, Ishida F, Umeda Y, et al. Low wall shear stress is independently associated with the rupture status of middle cerebral artery aneurysms. Stroke. 2013;44(2):519–21.
26. Frösen J, Tulamo R, Paetau A, et al. Saccular intracranial aneurysm: pathology and mechanisms. Acta Neuropathol. 2012;123(6):773–86.
27. Wang J, Wei L, Lu H, et al. Roles of inflammation in the natural history of intracranial saccular aneurysms. J Neurol Sci. 2021;424:117294.
28. Diagbouga MR, Morel S, Bijlenga P, et al. Role of hemodynamics in initiation/growth of intracranial aneurysms. Eur J Clin Investig. 2018;48(9):e12992.
29. Galis ZS, Sukhova GK, Lark MW, et al. Increased expression of matrix metalloproteinases and matrix degrading activity in vulnerable regions of human atherosclerotic plaques. J Clin Investig. 1994;94(6):2493–503.
30. Koseki H, Miyata H, Shimo S, et al. Two diverse hemodynamic forces, a mechanical stretch and a high wall shear stress, determine intracranial aneurysm formation. Transl Stroke Res. 2020;11(1):80–92.
31. Jeong W, Rhee K. Hemodynamics of cerebral aneurysms: computational analyses of aneurysm progress and treatment. Comput Math Methods Med. 2012;2012:782801.
32. Li Y, Corriveau M, Aagaard-Kienitz B, et al. Differences in pressure within the sac of human ruptured and nonruptured cerebral aneurysms. Neurosurgery. 2019;84(6):1261–8.
33. Shojima M, Oshima M, Takagi K, et al. Role of the bloodstream impacting force and the local pressure elevation in the rupture of cerebral aneurysms. Stroke. 2005;36(9):1933–8.
34. Hassan T, Ezura M, Timofeev EV, et al. Computational simulation of therapeutic parent artery occlusion to treat giant vertebrobasilar aneurysm. AJNR Am J Neuroradiol. 2004;25(1):63–8.
35. Cebral JR, Mut F, Raschi M, et al. Aneurysm rupture following treatment with flow-diverting stents: computational hemodynamics analysis of treatment. AJNR Am J Neuroradiol. 2011;32(1):27–33.
36. Suzuki T, Takao H, Suzuki T, et al. Determining the presence of thin-walled regions at high-pressure areas in unruptured cerebral aneurysms by using computational fluid dynamics. Neurosurgery. 2016;79(4):589–95.
37. Ban E, Cavinato C, Humphrey JD. Critical pressure of intramural delamination in aortic dissection. Ann Biomed Eng. 2022;50(2):183–94.

38. Ro A, Kageyama N. Pathomorphometry of ruptured intracranial vertebral arterial dissection: adventitial rupture, dilated lesion, intimal tear, and medial defect. J Neurosurg. 2013;119(1):221–7.
39. Mizutani T, Kojima H, Asamoto S, et al. Pathological mechanism and three-dimensional structure of cerebral dissecting aneurysms. J Neurosurg. 2001;94(5):712–7.
40. Mizutani T. Natural course of intracranial arterial dissections. J Neurosurg. 2011;114(4):1037–44.
41. Urasyanandana K, Withayasuk P, Songsaeng D, et al. Ruptured intracranial vertebral artery dissecting aneurysms: an evaluation of prognostic factors of treatment outcome. Interv Neuroradiol. 2017;23(3):240–8.
42. Amenta PS, Yadla S, Campbell PG, et al. Analysis of nonmodifiable risk factors for intracranial aneurysm rupture in a large, retrospective cohort. Neurosurgery. 2012;70(3):693–9.
43. Cornelissen BMW, Schneiders JJ, Potters WV, et al. Hemodynamic differences in intracranial aneurysms before and after rupture. AJNR Am J Neuroradiol. 2015;36(10):1927–33.